Juan Dong, Jeremy Epp, Robin Lipinski, Michael Sorg, Hans-Werner Zoch, Andreas Fischer

Combined X-ray diffraction and photothermal radiometry methods for in situ analysis of nitriding treatment

Journal Article	as:	published version (Version of Record)
DOI of this document*(secondary publication):		https://doi.org/10.26092/elib/3305
Publication date of this document:		13/09/2024

* for better findability or for reliable citation

Recommended Citation (primary publication/Version of Record) incl. DOI:

Juan Dong, Jeremy Epp, Robin Lipinski, Michael Sorg, Hans-Werner Zoch, Andreas Fischer, Combined Xray diffraction and photothermal radiometry methods for in situ analysis of nitriding treatment, Metall. Res. Technol. 115, 408 (2018). DOI: https://doi.org/10.1051/metal/2018045,

Metall. Res. Technol. **115**, 408 (2018)

https://doi.org/10.1051/metal/2018045

Metallurgical Research & Technology

Available online at:
www.metallurgical-research.org

Trends in heat treatment and surface engineering
Edited by Fabienne Delaunois, Véronique Vitry and Francine Roudet

Regular Article

Combined X-ray diffraction and photothermal radiometry methods for in situ analysis of nitriding treatment

Juan Dong[1,*], Jeremy Epp[1,3], Robin Lipinski[2], Michael Sorg[2], Hans-Werner Zoch[1,3], and Andreas Fischer[2,3]

[1] Leibniz Institute for Materials Engineering IWT, Bremen, Germany
[2] University of Bremen, Bremen Institute for Metrology, Automation and Quality Science, Bremen, Germany
[3] University of Bremen, MAPEX Center for Materials and Processes, Bremen, Germany

Received: 11 January 2018 / Accepted: 17 May 2018

Abstract. Monitoring the nitriding treatment by analyzing directly the components' surface state during the nitriding treatment is particularly interesting, since it allows a process monitoring and control based on the actual nitriding result. In the present study, two measuring methods are developed and combined with the aim of a direct surface state analysis during the nitriding treatment: the in situ X-ray diffraction (XRD) method and the photothermal radiometry. In order to validate the combined application of both methods during a nitriding treatment under controlled atmosphere, an experimental setup including a miniature nitriding furnace was developed. Two alloyed steels AISI 4140 and AISI H13 are treated with varying process atmosphere and nitriding potential leading to varying phase composition in the surface layer. As a result, the photothermal radiometry is shown to be sensitive with respect to the changing surface properties due to the growing compound layers and when porous layers are generated. It has a high potential to serve as surface sensor in industrial processes.

Keywords: nitriding / X-ray diffraction / photothermal radiometry / non-destructive testing / in situ analysis

1 Introduction

The nitriding treatment is widely used to obtain a compact compound (or nitride or white) layer and a deep diffusion layer on steel components. Actual methods for quality control are the analysis of the process atmosphere using gas sensors [1] during the process and the metallographic analysis after the process. However, the control of the process atmosphere not always guarantees that the desired nitriding result will be achieved [2]. In order to improve the process reliability, a surface sensor is required [3].

The photothermal radiometry is a capable candidate serving as surface sensor. It is a method for the noncontact and nondestructive measurement of surface layers. The measurement signals respond to the contrast of the thermal properties between the surface layers and the substrate. In the actual state, a reference method is needed to establish the correlation of the photothermal signal with the microstructure of the nitride layers. Therefore, the approach of the research work is the combined application of two in situ measuring methods, namely photothermal radiometry and in situ XRD. With XRD, reference information about the nature of the nitride layers and a qualitative evaluation of the layer thickness can be achieved in order to assess the photothermal signals. In this paper the combination of both methods for the real-time analysis of the surface layers during gaseous nitriding are presented. In the first step of the work, experiments have been carried out using laboratory equipment. Several results regarding the in situ measurements of nitride formation and nitride decomposition as well as the detection of insufficient nitride layer formation are finally demonstrated and discussed.

2 Photothermal radiometry

The photothermal method for the surface analysis involves the generation of thermal energy in the test object, e.g., by the absorption of a laser beam, as well as the detection of the resulting temperature changes, e.g., by means of infrared radiation, and the reconstruction of the thermal properties from the measured data [4]. The principle of a photothermal measurement on a coated sample is illustrated in Figure 1. An intensity modulated laser beam stimulates the object surface inducing thermal waves. They propagate to the layer/substrate interface [5] and are

* e-mail: dong@iwt-bremen.de

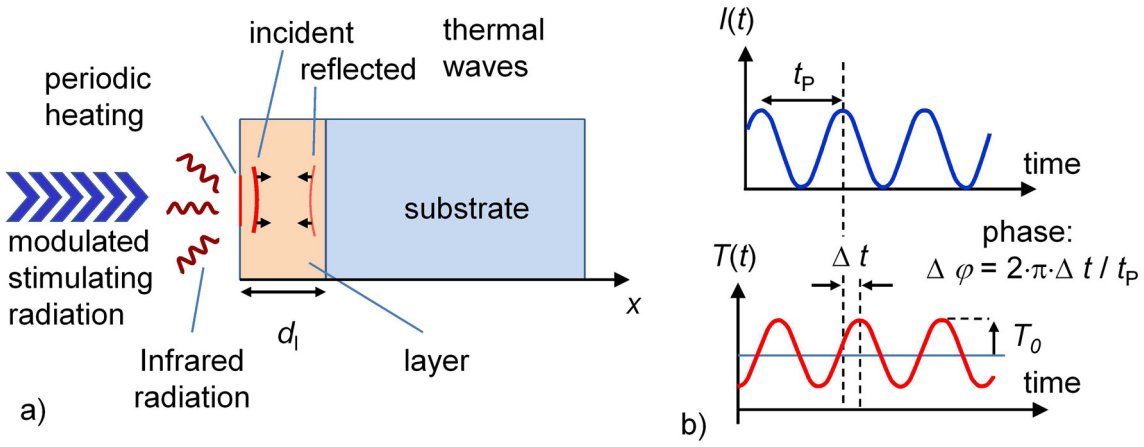

Fig. 1. Schematic illustration of the signal origin: a) stimulation and reflection of thermal waves in a coated sample; b) intensity-time curve of the stimulating radiation *I(t)* (top) and the resulting temperature-time curve *T(t)* of the surface (down).

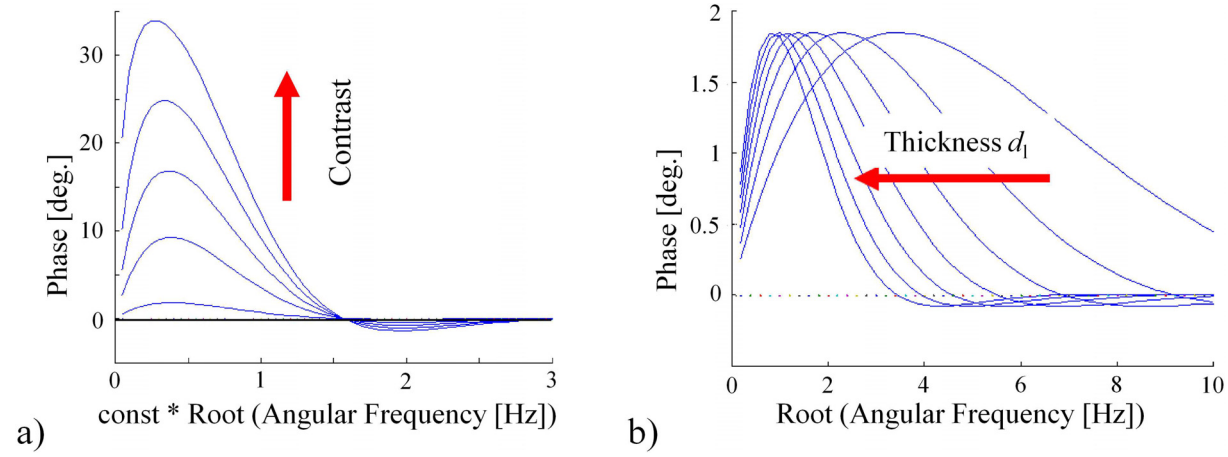

Fig. 2. Characteristic phase curves $\phi(\omega)$: a) phase curves for different R-values (contrast) with const $= d/(2\cdot\alpha)^{0.5}$; b) phase curves for different layer thickness d_l with constant R-value.

reflected back to the surface. Depending on the thermal diffusion length μ, the layer thickness d_l and the thermal reflection coefficient R, multiple thermal wave reflections occur. These waves result in an oscillating surface temperature, which is recorded by an infrared detector to obtain the temperature amplitude T_0 and the phase difference $\Delta\phi$ (with respect to the stimulating thermal wave).

In the one-dimensional case, thermal waves have a characteristic frequency-dependent thermal diffusion length μ [5]:

$$\mu = \frac{\lambda}{2\pi} = \sqrt{\frac{2\alpha}{\omega}}, \tag{1}$$

with:
– $\alpha = \kappa/(\rho c)$ = thermal diffusivity;
– λ = thermal wavelength;
– κ = thermal conductivity;
– ρ = density;
– c = specific thermal capacity;
– ω = angular frequency of stimulating wave;
– $\omega = 2\pi f$;
– f = stimulating frequency.

The thermal reflection coefficient R depends on the thermal contrast between the layer and the substrate, expressed via the ratio of their so-called thermal effusivities $E = (\kappa\rho c)^{0.5}$. Figure 2 illustrates typical diagrams, in which the phase signals are plotted vs. the square root of the frequency ($f^{0.5}$ or $\omega^{0.5}$). The phase maximum increases with increasing thermal contrast (Fig. 2a) and shifts to a lower frequency with increasing layer thickness at a constant thermal contrast (Fig. 2b) [6].

This behavior allows determining the thermal properties or the thickness of the layer from the value and the frequency position of the phase maxima respectively [7].

3 Experimental conditions

3.1 Specimens

A low alloyed steel and a middle alloyed steel were chosen as specimen material. The chemical compositions of the steels were analyzed by optical emission spectrometry

Table 1. Chemical composition of the steels AISI 4140 and AISI H13, balance Fe [mass-%].

	C	Si	Mn	P	S	Cr	Mo	Ni
AISI 4140	0.414	0.245	0.770	0.0087	0.0286	1.012	0.164	0.096
AISI H13	0.417	1.043	0.310	0.0200	0.0049	4.977	1.290	0.209

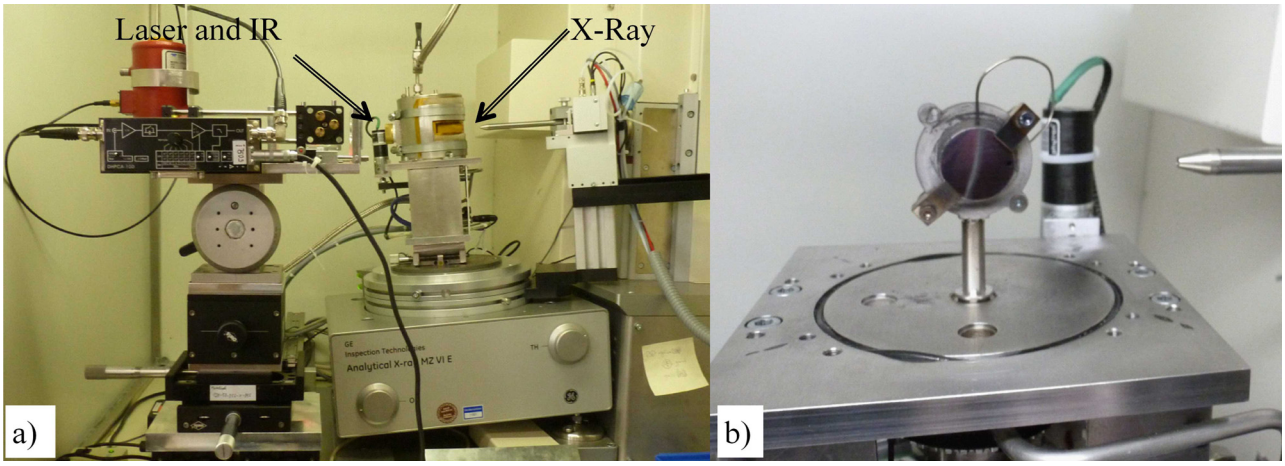

Fig. 3. Experimental chamber for in situ measurements: a) nitriding furnace (center), system for photothermal radiometry (left) and XRD measuring system (right); b) opened furnace and specimen with inserted thermocouple on the heating plate.

(OES) and are given in Table 1. Disk specimens of 5 mm in thickness and 25 mm in diameter were machined, martensitic hardened and tempered 2 h at 590 °C. The hardness was 342 ± 9 HV0.5 for the AISI 4140 steel and 572 ± 6 HV0.5 for the AISI H13 steel. Afterwards, the surface of the specimens was ground, lapped, polished and cleaned in a solvent-based cleaner. The specimens were stored in desiccators for 6 to 12 months. The surface state of the specimens is then defined as "passive". In addition to specimens with a passive surface state, several specimens were polished and cleaned again directly before nitriding. Such freshly created surface state is defined as "active".

3.2 Equipment

The experimental equipment consists of a self-built miniaturized nitriding furnace, a system for photothermal radiometry using a laser radiation with $\lambda = 975$ nm and a diffractometer (MZ VI E, GE Inspection Technology, Ahrensburg) (Fig. 3) using Cr-Kα radiation with $\lambda = 0.22909$ nm and a Position Sensitive Detector (PSD). The furnace has a sapphire window and a polyimide window. The window materials are transparent for infrared radiation and for X-ray respectively. For the in situ XRD measurement of the nitride layers at elevated temperature, it should be considered that the diffraction peaks shift their angular positions from the standard patterns more or less depending on the temperature, on the real nitrogen content in nitride and on the residual stress in the phases [8–10].

The furnace is equipped with a heating plate with specimen mounting parts, flow meters for process gases (NH_3, N_2, H_2), thermocouple for temperature regulation, hydrogen- and oxygen-sensor for determination of nitriding potential (K_N), as well as a control unit for programming processes and recording process data.

The photothermal and XRD measurements were conducted alternatively (quasi-simultaneously) within a timeframe of about 3 minutes and 5 minutes respectively.

3.3 Processes

The parameters of three nitriding experiments are given in Table 2. Process 1 was performed in three steps: step 1 was used in order to supply the reference condition at 550 °C in N_2 immediately before nitriding, step 2 served to measure the development of nitride layer during nitriding in NH_3 and step 3 was used to characterize the decomposition of nitride in N_2 after nitriding. Additionally, two processes (2, 3) were conducted with a constant incoming gas mixture ($NH_3 + N_2 + H_2$), which was chosen to establish the nitriding potential $K_N = 2$ by means of preliminary experiments. The specimen and the furnace were cooled in N_2 from 550 °C down to 60 °C after the process. It should be mentioned that the addition of NH_3 into the process atmosphere during heating is necessary to avoid passivation of the steel surface, especially for polished AISI H13.

4 Results and discussion

4.1 In situ measurements on steel surface during nitriding and denitriding

Process 1 (as mentioned above, Table 2) was designed to distinguish the features of the photothermal signals in different conditions of steel AISI 4140 by three process steps:

Table 2. Parameters of the nitriding processes.

Process	Steel grade	Heating, 50–550 °C	Process step, 550 °C		
			Holding	Nitriding	Denitriding
1	AISI 4140	In N_2	37 min in N_2	30 min K_N8 + 170 min K_N5 in NH_3	117 min in N_2
2	AISI H13	In $NH_3 + N_2 + H_2$	–	120 min K_N2 in $NH_3 + N_2 + H_2$	–
3	AISI H13	In $NH_3 + N_2 + H_2$	–	180 min K_N2 in $NH_3 + N_2 + H_2$	–

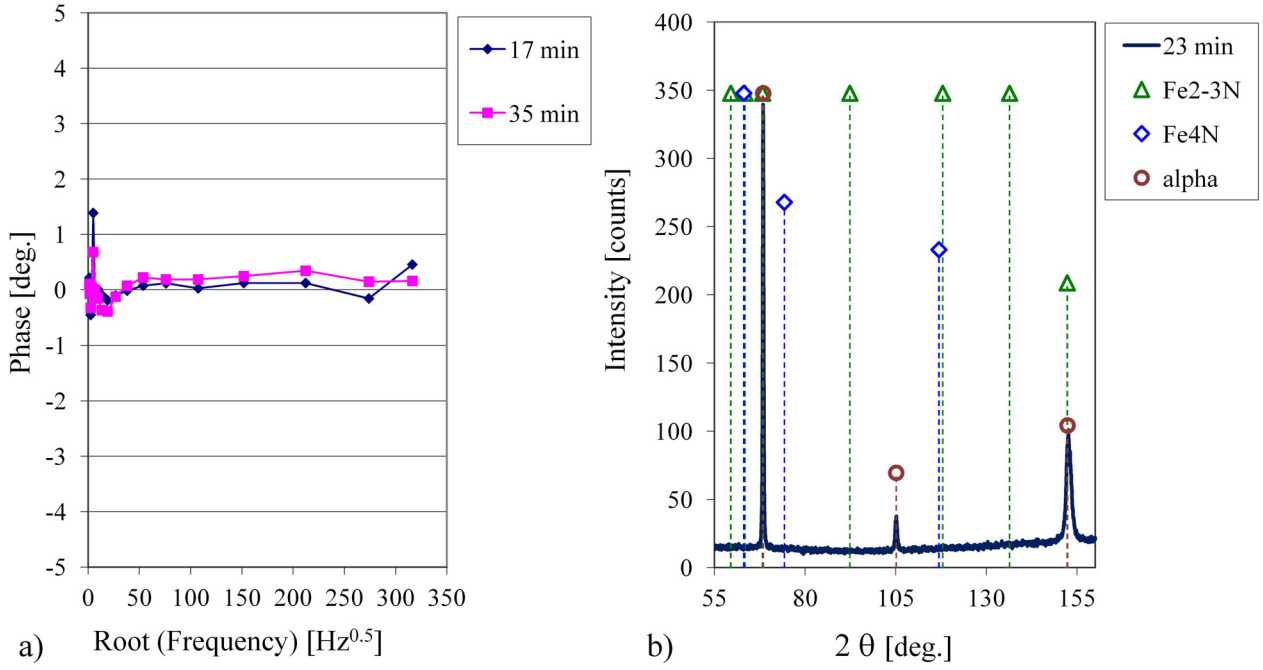

Fig. 4. Measured signals for the surface on steel AISI 4140 in N_2 at 550 °C prior to nitriding: a) photothermal phase curves; b) XRD diagram (process 1, step 1).

– step 1: specimen in nitrogen gas at elevated temperature immediately before nitriding (homogeneous surface state);
– step 2: nitride formation and growing with increasing nitriding duration;
– step 3: nitride decomposition in nitrogen gas after previous nitriding process step.

As reference, the surface state of the specimen at 550 °C in N_2 was measured (Fig. 4) before nitriding in process step 1. The two photothermal phase curves (Fig. 4a) were plotted from the data from the second and the third measurements minus the data from the first measurement serving as the reference. The two phase curves run parallel to the abscissa near zero degree, which means that no change (compared to the substrate) of the thermal properties was detected. The XRD diagram (Fig. 4b) confirms that only α-Fe, with three associated diffraction peaks ({110}α at 68.4 deg.; {200}α at 105.1 deg. and {211}α at 152.3 deg.), are present. The angle positions of the diffraction peaks show displacements compared to those of iron powder in standard of ICDD, PDF Database (ICDD the International Centre for Diffraction Data: 01-071-4648) because of the thermal expansion.

The average values of the photothermal phase data serve as reference and were subtracted from the data of all following measurements on steel AISI 4140. This is necessary to eliminate the transfer function of the measuring electronics.

In process step 2, the nitriding process began shortly after changing the incoming gas from N_2 to NH_3. A high flow rate of NH_3 was applied for 30 min to improve the nucleation of nitride on steel surface. The flow rate of NH_3 was then reduced to a lower level for about 170 min. The resulting nitriding potentials were about $K_N = 8$ and $K_N = 5$, respectively.

The photothermal diagrams (Fig. 5a) show that a phase maximum appeared already on the first curve 17 min after supplying NH_3 gas. The phase maximum shifts continuously to lower frequencies with increasing time down to ca. 38 $Hz^{0.5}$ and the value of the phase maximum increases up to ca. 11 deg at 190 min. The results indicate that a nitride layer is formed and the layer thickness increased with the

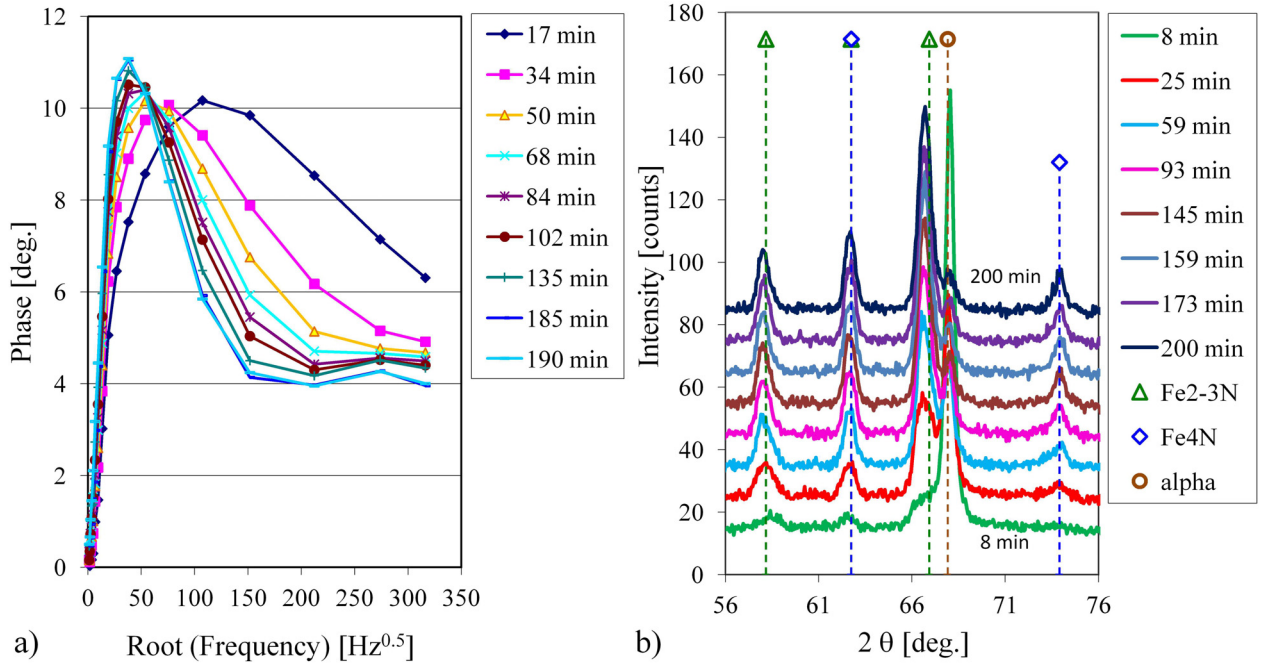

Fig. 5. Measured signals for the surface on steel AISI 4140 during nitriding at 550 °C with K_N 8/5: a) photothermal phase curves; b) XRD diagrams (process 1, step 2).

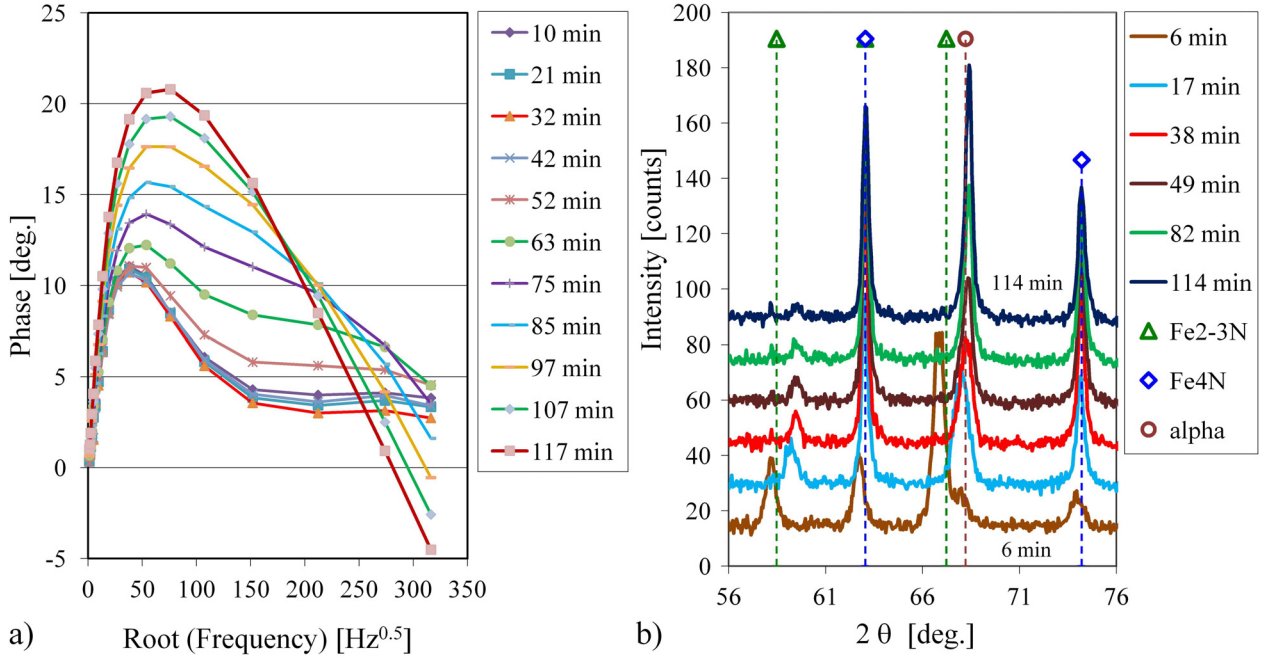

Fig. 6. Measured signals for the surface layer on steel AISI 4140 during holding in N_2 at 550 °C after nitriding: a) photothermal phase curves; b) XRD diagrams (process 1, step 3).

time. The nitride layer has a lower thermal diffusivity than the substrate and the thermal contrast increased slightly with the increasing nitriding duration [6].

The corresponding XRD diagrams (Fig. 5b) show the diffraction peaks of γ'-Fe_4N and ε-$Fe_{2\text{-}3}N$ evidently. The intensity of the nitride peaks increased with increasing time, whereas the intensity of α-Fe peak coming from the region below the compound layer decreased, which confirms the growing of the layer thickness during the process. These results correlate well with the interpretation of the photothermal measurements that the compound layer is formed and the thickness grows with the nitriding time.

After completing the step 2 of the process, step 3 (denitriding for 117 min) was started by changing the incoming gas from NH_3 to N_2.

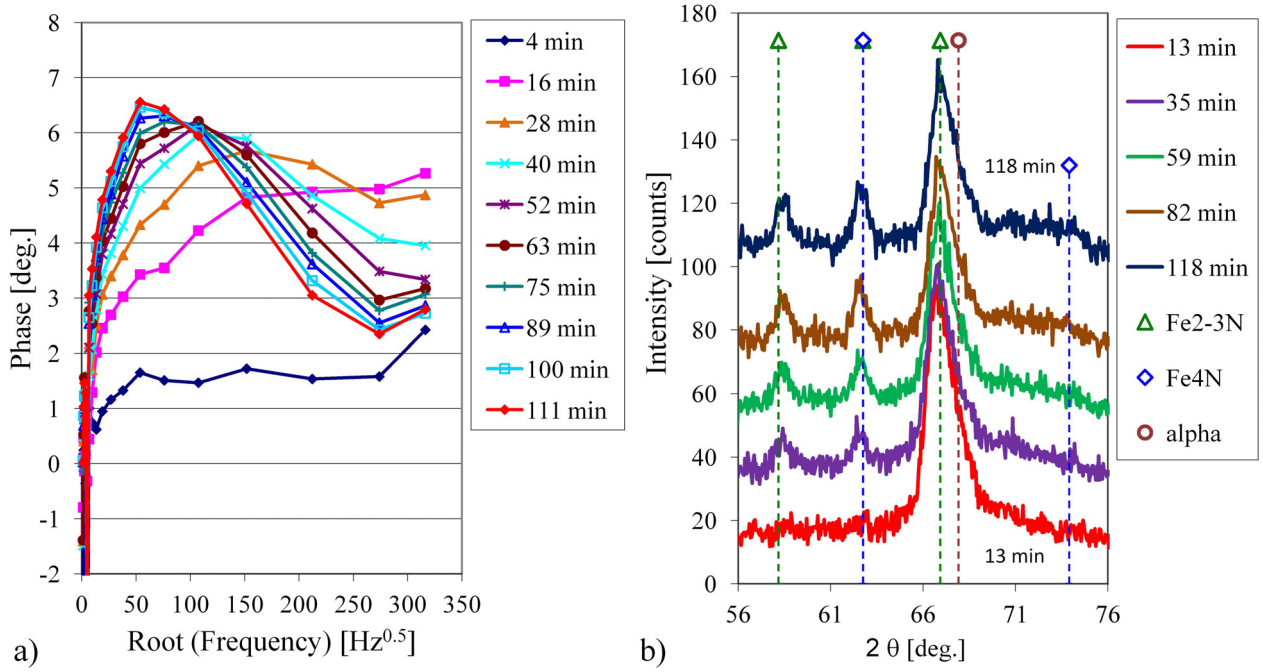

Fig. 7. Measured signals on steel AISI H13 with an active surface during nitriding with $K_N = 2$ at 550 °C: a) photothermal phase curves; b) XRD diagrams (process 2).

Within the first 32 minutes, the photothermal phase signals (Fig. 6a) lowered slightly, thereafter the phase maxima raised strongly. By comparison with Figure 2a, it can be concluded that the thermal contrast between the surface layer and the substrate decreased first slightly and then increased strongly.

The XRD diagrams in Figure 6b exhibit two-stage changes as well:

– (1) the shift of the diffraction peaks of ε-Nitride to a higher 2θ −angle (lower d-value), the reduction of the ε-Nitride intensity and the increase of the γ'-Nitride intensity in the first stage within 38 min;
– (2) the continual decrease of the ε-Nitride intensity, the increase of the γ'-Nitride intensity and especially the increase of the α-Fe intensity in the second stage up to 114 min.

The shift of the ε-Nitride peaks indicates clearly the reduction of the nitrogen concentration in the phase. The γ'-Nitride peaks shifted as well but only slightly, and the shifts can hardly be noticed. The result demonstrates the evidence that ε-Nitride is transformed to γ'-Nitride firstly and γ'-Nitride is transformed to α-Fe lately. Furthermore, the nitrogen atoms released from the nitrides recombine with each other to molecular nitrogen [11].

It can be concluded from Figure 6 that the transformation of ε-Nitride to γ'-Nitride is responsible for the reduction of the thermal contrast in the first stage of the denitriding, while the transformation of γ'-Nitride to α-Fe cannot be responsible for the increase of the thermal contrast in the second stage of the denitriding, as the original phase shift produced by α-Fe should be 0 deg. The reason for the strongly increasing phase shift could be attributed to the pore formation, which was proved by microscopic analysis [12]. Indeed, the pores have a low thermal conductivity and built an additional layer at the top of the compound layer.

4.2 Detection of insufficient nitride formation in process

Process monitoring includes the prevention of an insufficient formation of the nitride layer. This was checked for nitriding processes on steel AISI H13 in different surface state condition. The hot forming tool steel tends to have a passive surface state caused by the natural formation of a thin oxide layer. The passive surface layer can block the nitride formation in the nitriding processes. Two nitriding experiments were conducted respectively on an active specimen and a passive specimen. The active specimen was polished freshly before nitriding and the passive specimen was polished and stored 6 months in air before nitriding.

Figure 7 shows the measured diagrams of the active specimen. At the surface, a nitride layer (compound layer) is formed according to the nitride diffraction peaks in the XRD diagrams. The photothermal phase curves show a similar typical shape while the nitride layer is formed on the steel surface, which was described previously for the steel AISI 4140. A post-process microscopic analysis proved that a compound layer with 3 µm in thickness and a precipitation layer with about 70 µm in thickness below the compound layer occur in the steel surface.

Figure 8 shows the measured diagrams during the process with the passive specimen. No obvious nitride diffraction peaks, but only α-Fe peaks, can be identified in the XRD diagrams. Merely a very small Fe_4N peak at 63°

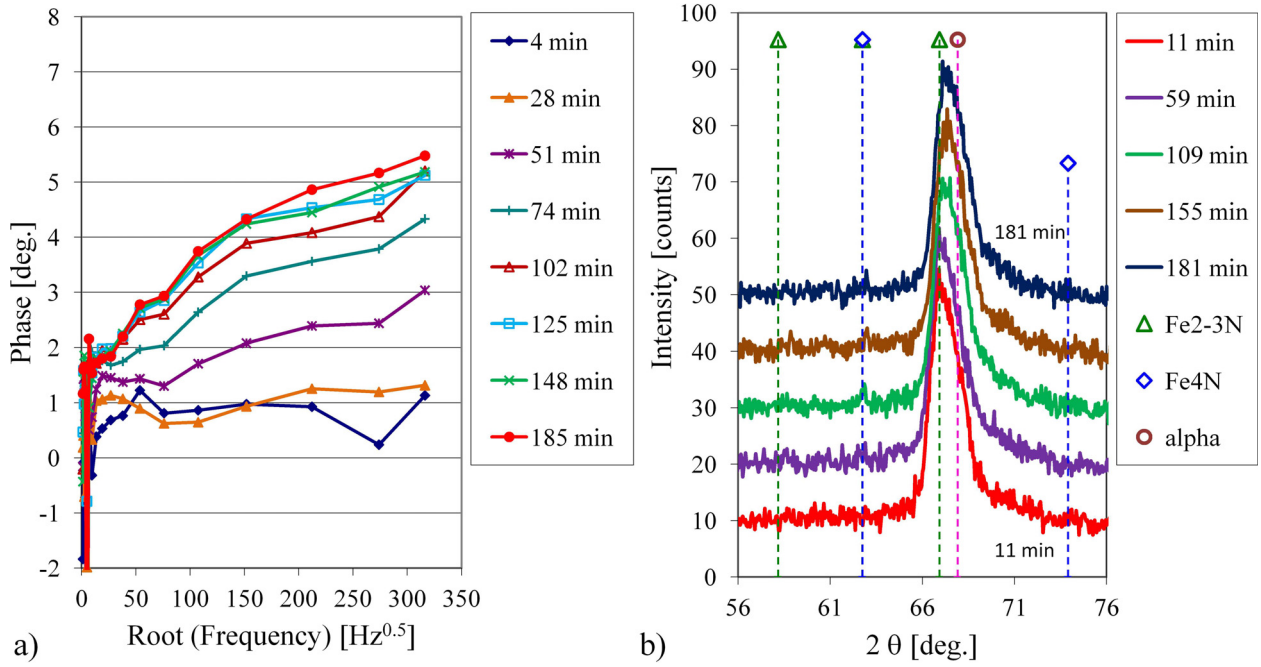

Fig. 8. Measured signals on steel AISI H13 with a passive surface during nitriding with $K_N = 2$ at 550 °C: a) photothermal phase curves; b) XRD diagrams (process 3).

and 75° might be suspected towards the end of the process. The photothermal phase curves exhibit an unusual shape with sloped lines while a comparable maximal phase signal as reached for the active sample (Fig. 7a) is observed at high frequencies ($> 250\,\mathrm{Hz}^{0.5}$) by the end of the process. This indicates that a very thin compound layer could be found on the surface as supposed by the XRD diagrams. The result distinguishes from the case of a successful nitrided steel surface with a complete compound layer (Fig. 7a). A microscopic analysis proved that the nitride layer was formed at a small part of the specimen surface. There are however areas without any compound layer and with only a very thin inhomogeneous precipitation layer.

In conclusion, the experimental results confirm that the photothermal measuring technique has the capability for the online monitoring of the nitriding process regarding the nitride layer development in real-time.

5 Summary and outlook

In the present work, a photothermal method was developed and tested for the in situ monitoring of the nitride layer formation during the nitriding process. For this purpose, photothermal measurements were applied in combination with XRD measurements during nitriding processes. As a result, the correlation of the photothermal phase signal to the nitride layer formation was validated by the XRD method. The experiments were conducted in a self-developed miniature nitriding furnace, which allows the combined application of the two measuring techniques.

The results show that the photothermal radiometry is sensitive to changes of the thermal surface properties due to the growing compound layer and when porous layers are generated. The occurrence of phase maxima in the phase-frequency diagrams correlates with the formation of the compound layer via the change of thermal diffusivities. The frequency positions of the phase maxima relate to the layer thickness. In order to obtain quantitative information of the layer thickness, a calibration of the measurement system is required, which will be addressed in future investigations.

The performed experiments also allow gaining knowledge about the ongoing mechanisms during the denitriding of the layer. The denitriding occurred in two stages:

– 1) reduction of the nitrogen concentration within ε-Nitrid and ε-Nitrid transformation in γ'-Nitrid;
– 2) γ'-Nitrid transformation in α-Fe and pore formation. The first stage leads to slight lowering of the thermal contrast, which increases strongly in the second stage caused by pore formation.

The performed study shows that the combined methods of XRD and photothermal radiometry are useful for the analysis of nitriding processes regarding unanswered questions concerning the grow kinetics of compound layer, the surface passivation as well as the pore formation. The photothermal radiometry has a high potential to be used as surface sensor in industrial processes.

Acknowledgements. The IGF Project (18306 N) of the Arbeitsgemeinschaft Wärmebehandlung und Werkstofftechnik e. V. (AWT) was funded by the Arbeitsgemeinschaft industrieller Forschungsvereinigungen "Otto von Guericke" e. V. (AiF) through the IGF program of the Bundesministerium für Wirtschaft und Energie (BMWi) due to a resolution of the Deutscher Bundestag. The authors are grateful for the financial support.

We further wish to thank the Expert Committee 20 "Sensors in heat treatment" of AWT for scientific support and supervision of the project. Our special thank is given to the members of the Board of Experts for their collaboration and interest in the project: Process-Electronic GmbH, Stange Elektronik GmbH, KGO GmbH and Ipsen international GmbH.

References

1. D. Liedtke, H. Altena, Über die Prozessregelung beim Gasnitrieren und Nitrocarburieren in der Praxis, ATTT-AWT-SVW-VWT-Tagung, Nitrieren, Aachen, DE, 10–12 Apr, 2002, pp. 351–367
2. B. Haase, Qualitätssicherung in der Oberflächentechnik. Qualifizierungsinitiative Oberflächentechnik – Qualifizierungsnetze im Norden Deutschlands; Tagungsband des VDI-TZ und der TuTech am 20.02.2001 in Hamburg. Düsseldorf, Oktober 2001, ISSN 1438-1389, pp. 49–68
3. H. Klümper-Westkamp, F. Hoffmann, P. Mary, B. Edenhofer, In-situ monitoring of layer formation, case depth and phase composition during nitriding and nitrocarburising, Heat Treat. Met. **4**, 112–118 (1992)
4. H.S. Carlslaw, J.C. Jaeger, Conduction of heat in solids, Oxford University Press, U.S.A., 1959
5. A. Rosencwaig, Photoacoustics and photoacoustic spectroscopy, Wiley, New York, 1980
6. C.A. Bennett, Jr., R.R. Patty, Thermal wave interferometry: A potential application of the photoacoustic effect, Appl. Opt. **22(1)**, 49–54 (1982)
7. G. Goch, Zerstörungsfreie Randzonenanalyse von Freiformflächen und strukturierten Oberflächen, in: Prozessketten zur Replikation komplexer optischer Komponenten, Transregionaler Sonderforschungsbereich TR4 der Deutschen Forschungsgemeinschaft (DFG), Abschlussbericht, 2012, pp. 389–412
8. U. Schlaak, T. Hirsch, P. Mayr, Röntgenographische in-situ-Messungen zum thermischen Eigenspannungsabbau bei erhöhter Temperatur, HTM **43(2)**, 92–101, 1988
9. H. Oettel, B. Ehrentraut, Makroskopische Eigenspannungen in der Verbindungsschicht gasnitrierter Stähle, HTM **40(4)**, 183–187, 1985
10. U. Kreft, F. Hoffmann, T. Hirsch, P. Mayr, Formation of residual stresses in compound layer during gas nitriding measured by in-situ technique, Surf. Eng. **11(1)**, 61–65, 1995
11. S. Pietzsch, S. Böhmer, Erscheinungsformen der Porosität nitridischer Verbindungsschichten, HTM **49(3)**, 168–175, 1994
12. J. Dong, H. Prekel, M. Dethlefs, J. Epp, A. Fischer, In-situ investigation of surface layers during gaseous nitriding by means of XRD and photothermal radiometry, HTM J. Heat Treat. Mater. **72(3)**, 154–167, 2017

Cite this article as: Juan Dong, Jeremy Epp, Robin Lipinski, Michael Sorg, Hans-Werner Zoch, Andreas Fischer, Combined X-ray diffraction and photothermal radiometry methods for in situ analysis of nitriding treatment, Metall. Res. Technol. **115**, 408 (2018)